

Experimental Performance Evaluation of Ventilated Mixers— A New Mixer Concept for High-Bypass Turbofan Engines

J S Sokhey*

Boeing Commercial Airplane Company, Seattle, Washington

The experimental performance data and analysis from a dual cold/hot flow nozzle test on two ventilated mixer models is presented. The test measurements include total axial nozzle thrust, surface static pressures, and rake surveys of total pressure and total temperature taken at the charging station, the mixing plane, and the nozzle exit plane. The mixer models were designed and developed using computational techniques. A special numerically controlled manufacturing technique was used in fabricating the mixer hardware. Ventilation slots through the lobe walls were machined to inhibit separation by energizing the boundary layer in the primary flow. The analyses of the test results on ventilated mixers, as compared to the corresponding unventilated mixers, indicate that the ventilation concept results in a significant reduction in total mixer pressure loss, decrease in jet noise, and increase in mixing effectiveness. The characteristics of mixer ventilation and its impact on a current technology turbofan engine is also investigated.

Nomenclature

C_D	= nozzle discharge coefficient
C_V	= nozzle velocity coefficient
F	= thrust
L	= axial length
P	= static pressure
P_t	= total pressure
T_t	= total temperature
W	= air flow rate
η	= mixing effectiveness
<i>Subscripts</i>	
exit, e	= nozzle exit quantity
F	= fan flow
M	= fully mixed flow (also mixing plane station)
Mea	= measured quantity
p	= primary flow
PM	= partially mixed
tot	= total quantity

Introduction

FORCED mixing for use in turbofan engines has received considerable attention recently as a means of noise reduction as well as thrust augmentation. The theoretical potential in fuel savings, especially in high bypass engine cycles is sufficient to warrant an extensive research effort. However, in practice mixers have performed well below expectations. Test results have failed to demonstrate mixers as a practical means of improving the performance of turbofan engines. The reasons for this failure are twofold: first, the implementation of a mixed flow long duct nacelle on aircraft has resulted, to date, in weight and drag penalties which eliminate most of the potential gains of a mixed flow cycle; second, the internal performance of the mixer has produced less mixing than expected, while introducing more losses than anticipated.

Much of the research in mixer technology consists of experimental studies evaluating the effect of mixer parameters on overall performance. Consequently, the design techniques depend considerably on empirical data in developing improved high performance mixers. References 1-4 describe some of the recent experimental and theoretical work on mixers. To develop an efficient mixer with minimal pressure loss, it is necessary to study the flow through the mixer passages where the flow is highly nonuniform and three dimensional in nature. The current mixer designs are based on parametric studies where the performance effects of geometrical parameters (Fig. 1) are evaluated separately. The experimental results from mixer tests have shown that geometrical parameters which enhance mixing also introduce additional losses in the flowfield as a result of skin friction, flow turning, and boundary-layer separation. In lobe mixers for high bypass ratio engines, boundary layer separation has been the source of large pressure losses in the primary flow passages. Kuchar and Chamberlin¹ have shown experimentally that the amount of penetration of mixer lobes into the secondary flow is directly proportional to the degree of mixing. However, as the lobe penetration (Fig. 1) increases above 40%, the boundary layer separation occurs in the primary flow due to excessive turning. The separation loss has been found to occur even when the lobes are scalloped or cut back to increase mixing.^{1,3} Similar results were also found earlier in this investigation (1979) when a series of wind tunnel tests employing plexiglas mixer lobes was conducted. The plexiglas mixer models were used to facilitate the observation of flow visualization patterns on mixer surfaces. The existence of flow separation inside the lobe was confirmed by the analysis of surface flow patterns and total pressure measurements.

The current investigation of ventilated mixers is directed at improving overall mixed flow performance by designing compact mixers which efficiently reduce mixer pressure loss, enhance mixing effectiveness, and reduce jet noise as well.

Development of Ventilated Mixers

The concept of mixer ventilation was developed as a means of energizing the boundary layer in the region prior to the point of separation (Fig. 2) so that separation is inhibited. The ventilation was achieved by placing slots through each lobe surface. However, proper location, design size, and orientation

Presented as Paper 82-1136 at the AIAA/SAE/ASME 18th Joint Propulsion Conference, Cleveland, Ohio, June 21-23, 1982; received Nov. 19, 1982; revision received April 24, 1984. Copyright © American Institute of Aeronautics and Astronautics, Inc. 1984. All rights reserved.

*Senior Specialist Engineer, Nacelle Aerodynamics Research.

tation of ventilation slots is essential for the success of this concept

An experimental study to investigate and optimize the ventilated mixer concept⁵ was conducted in 1979-1980. The objectives of the study were 1) to detect and locate the regions of flow separation, 2) to investigate other high pressure loss regions inside the mixer lobes, and 3) to evaluate the ventilated mixer concept as a means of eliminating separation and related pressure loss.

The mixer models were fabricated from a 1/8 in.-thick plexiglas sheet to facilitate flow visualization. The models varied in length and flow turning, so as to represent some of the common high bypass mixer designs. Each of the mixer models consisted of a single lobe crown and the two lobe valleys. This design allowed a close focus on the region where the mixer passage loss is most likely to occur. The lobe models were designed to simulate the primary and the secondary flow streams of a full scale mixer lobe for a turbofan engine with the bypass ratio of two.

The occurrence of flow separation on the primary surface of the lobe was observed from surface oil flow patterns. The flow pattern for an unventilated lobe (Fig. 3a) illustrates the occurrence of reverse flow or flow stagnation (indicated by dots) on the primary side. The ventilation slots (Fig. 3b) cause the flow to remain attached to the surface by energizing the boundary layer near the lobe crown.

As further evidence of flow separation, two different techniques were used in the measurement of total pressure at the mixing plane. Figure 4a presents the total pressure field plots obtained by a photographic technique developed by Crowder⁶ where an oscillating pitot probe senses local total pressure. Four different dynamic pressure levels can be distinguished by this method when the recording is done on a color film. Darker levels of shade represent a larger drop in total pressure. Figure 4b presents a plot of total pressure along the lobe crown and valley centerlines. The portions of the total pressure curves associated with separation are indicated by large pressure drops with a transient flow behavior. A buildup of low energy boundary layer in the lobe valley and at the bottom of the lobe is also indicated. The ventilation was found to eliminate separation and associated pressure loss, as indicated in Fig. 5.

The final slot ventilation configuration for optimum performance was obtained after a series of optimization experiments where a number of mixer models, covering a matrix of slot ventilation parameters such as the width and length of each slot, axial location of slots with respect to the lobe axial station, number of slots required per lobe, and orientation of the slot at its entry and exit through the lobe wall, were tested.

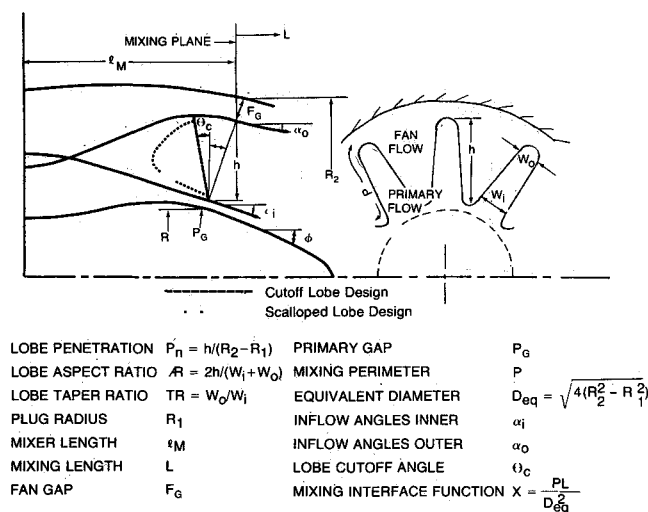


Fig 1 Mixer geometrical parameters

Test Rig and Facility

The mixed flow nozzle tests were conducted in the Boeing Nozzle Test Facility (NTF), Cell 2 in Seattle. The model was tested on Nozzle Test Rig A, a dual hot/cold test facility (Fig. 6) which measures axial static thrust up to 1600 lb. A 6 in. propane burner attached to the rig provides hot primary flow with average flow temperatures of 1500 R. The data acquisition and reduction system computes on line the burner fuel/air ratio, the burner efficiency, and the heated air temperature.

Instrumentation

The instrumentation required includes devices for measuring temperature, total pressure, and static pressures at selected stations along the mixed nozzle axis. The pressure measurements, except for the reference ambient pressure, were taken using Statham (or equivalent) differential transducers. The ambient pressure was measured by a Rosemount 15 psia transducer. Five 48 port scanivalves were used to record pres-

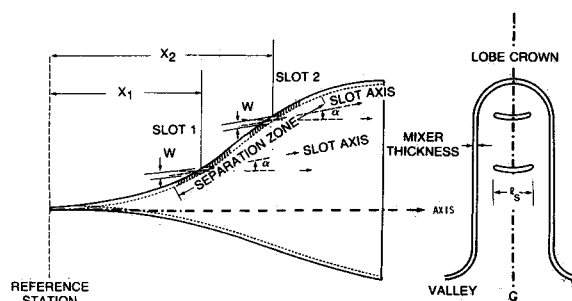


Fig 2 Ventilated mixer geometry

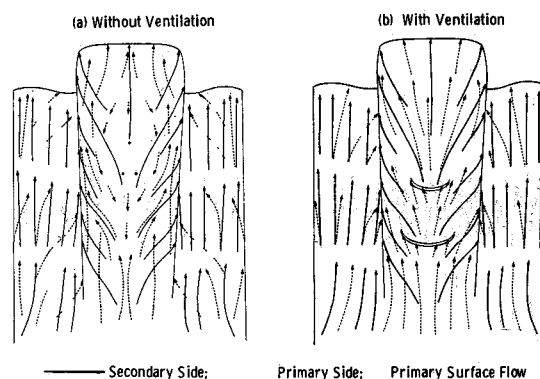


Fig 3 Surface flow on mixer lobe surfaces (top view)

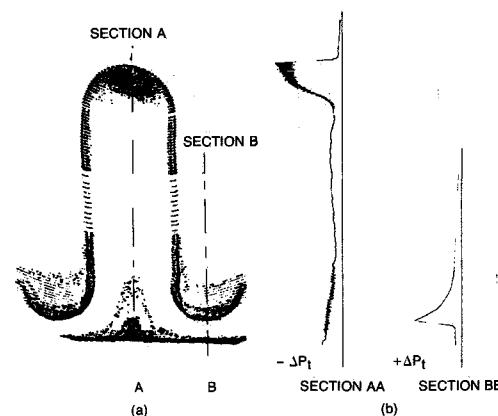


Fig 4 Total pressure plots at the mixing planes

tures—two each for recording charging station total pressures and static pressures in the primary and the secondary flow streams, respectively, and one for recording the mixing and the exit plane rake total pressures. Chromel alumel thermocouples were employed to measure the temperature. The instrumentation on the test facility was required to calculate axial thrust, balance temperature, stream static pressure, and additional pressure and temperature measurements used to evaluate axial force sensitivity and pressure tare corrections.

The airflow measurement was obtained with a set of multicritical flow venturis (MCV's) installed in the primary and the secondary supply systems. Depending upon the amount of airflow, the system selects an appropriate venturi for passing the air supply. The flow rate calculation employed suitable flow constants and calibration curves obtained prior to this test.

A new rotating mechanism for rake surveys was fabricated. It consisted of rotating the entire fan cowl/nozzle with the mixing and the exit plane rakes fixed to it through a 30 to 45 deg sector using a set of Globe motors and a gear chain. The mixing plane rakes consisted of a total pressure rake and a total temperature rake situated diametrically opposite. At the

nozzle exit, total temperature and total pressure probes were placed on a single rake spanning the exit diameter, with the total pressure probes located in one half and the total temperature probes located in the other half. The nozzle exit survey rake was offset by 90 deg to the mixing plane rakes, so that the exit data was uninfluenced by mixing plane instrumentation. At the beginning of the test, a circular scale and an inclinometer were used to calibrate the potentiometer and, hence, the angular rotation of the rakes. The model assembly and the instrumentation are shown in Fig 7.

Data Reduction

The transducer data for selected steady state conditions through a set of signal conditioners was acquired by an 80-channel HP-3495A data scanning computer. An HP 9825A desk top computer was used to control HP 3495A, store the data in engineering units on a cassette tape, and also transmit it to the ECLIPSE S 130 computer for further data reduction. In addition, realtime data monitoring on a CRT display was used to allow a closer control over test conditions.

The ECLIPSE computer performed the on line data reduction using area-weighted, effective charging station pressure in the calculation of nozzle performance parameters. The performance data was subsequently reprocessed off line, using area weighted temperature averaging.

Model Description

A schematic diagram of the model configurations is presented in Fig 8. The six model configurations tested were 1) simple splitter/short pointed plug, 2) long unventilated mixer/long plug, 3) short unventilated mixer/short plug, 4) long ventilated mixer/long plug, 5) short ventilated mixer/short plug, and 6) simple splitter/short plug.

The length of the mixing chamber (L/D) in all the mixer configurations is kept constant (0.65). Test configurations 4 and 5 were obtained by ventilating the mixer models tested in configurations 2 and 3 (see Fig 8). The ventilation slots allowed the fan flow to bleed into the primary flow, thus energizing the primary flow boundary layer near the lobe crowns. The ventilation was found to increase the bypass ratio of the mixed flow system by about 3 to 4%. Figure 9 presents a typical test configuration.

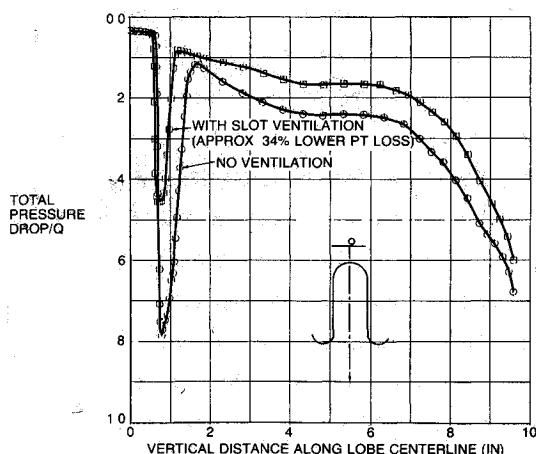
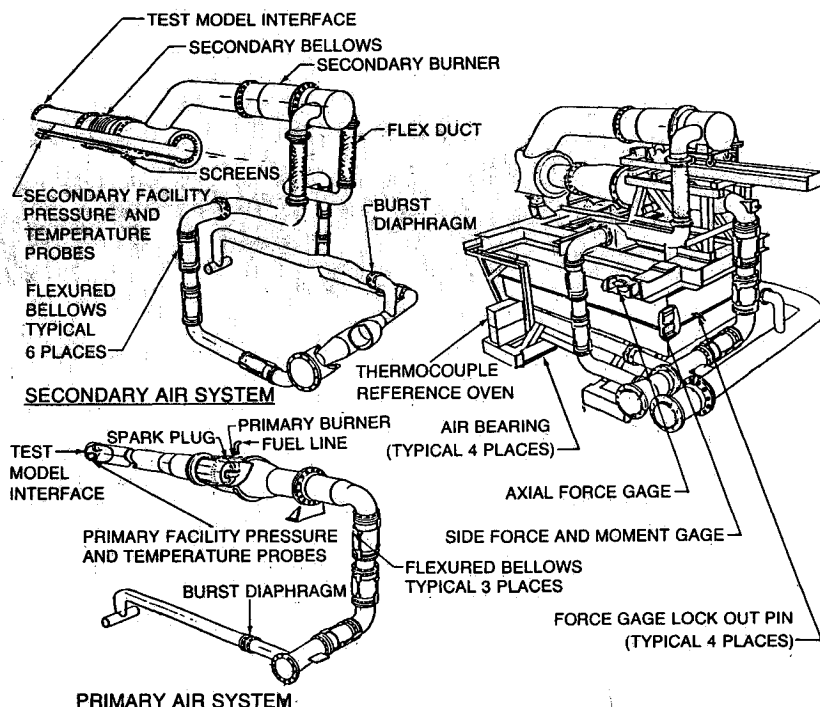


Fig. 5 Reduction in pressure loss due to ventilation

Fig 6 Nozzle test facility—thrust, Rig A.



Mixer Design and Fabrication

Two mixer models were computer designed and lofted using a bicubic geometry development system. Each mixer was fabricated from a single stainless steel block using a special procedure developed to machine the mixer surface contours. This state of the art procedure, though expensive, was chosen to develop the new technology and to fabricate mixer models which were aerodynamically smooth in the lobe entrance region.

A preliminary mixer design was obtained from previous parametric studies. During the subsequent design process, some of these parameters were modified to provide an efficient flow through the mixer, but the basic features such as number of lobes, lobe penetration, lobe shape, etc., were preserved. The design of mixer flow areas, surface contours, and length required an iterative procedure which matched the lobe passage design, based on the desired cross-sectional shape, with the design obtained through fluid flow analysis of the mixer duct. Detailed description of lobe surfaces was obtained computationally through the use of a bicubic geometry system program called MASTER⁷ where the surfaces are represented by sets of four sided parametric cubic patches covering the entire surface of the mixer lobes. This system allowed modifications to the geometrical input by examining the surfaces with the help of video-graphical monitors or by analyzing the data information on surface derivatives. Special techniques were used to design and develop local surface regions where large curvatures, in flexion points, etc., may occur. The procedure discussed above is summarized in the flow chart (Fig. 10).

A new manufacturing technology for fabricating the lobe mixers was developed and used on these models. The process

consisted of using numerically controlled (NC) machines for building specially designed electrodes, and using these electrodes for machining the surface contours of the mixer lobe by an electrical discharge (EDM) process. The EDM process was selected since the mixer size or scale was small, and because of the relatively thin lobe walls. Conventional NC machining techniques would require miniaturized cutting tools, sufficient spatial movement for tool orientation along the machining surface, and adequate access space to the entire machining surface. Perhaps the most important reason for selecting the EDM process was that the thin mixer walls would be subjected to pressures too excessive for them to remain rigid during the machining process. This process was very time consuming and expensive; however, the reproduction of the surface contours was found to be accurate to within 0.005 in. of the specified surface coordinates. Each mixer model consisted of 12 identical lobes; therefore, only one set of electrodes was required for fabricating each mixer configuration.

Test Procedures

The test was conducted between December 8, 1980 and February 11, 1981. It consisted of axial thrust measurements, surface static pressure measurements, total pressure and total

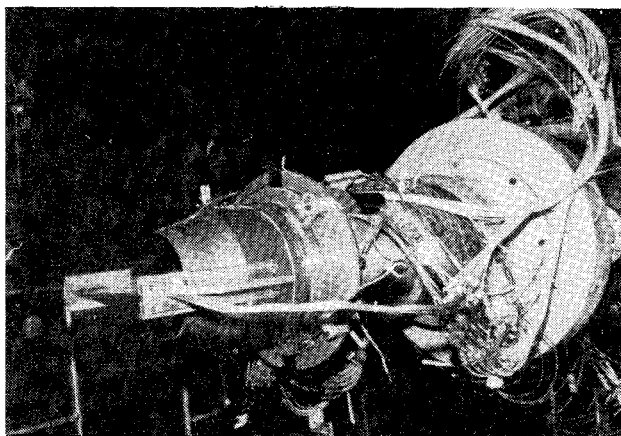


Fig 7 Model assembly and instrumentation

MIXER LENGTH	$(L_M/D)_1 = 0.37$	$(L_M/D)_2 = 0.27$
LOBE PENETRATION	$PEN_1 = 59\%$	$PEN_2 = 61\%$
MIXER CHAMBER LENGTH	$(L/D)_1 = 0.64$	$(L/D)_2 = 0.64$

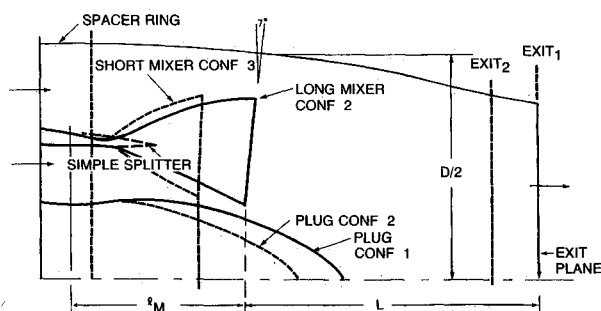


Fig 8 Mixed flow configurations

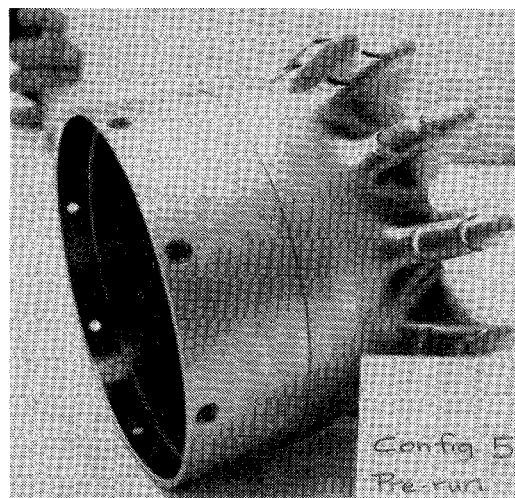


Fig 9 Mixer test—Configuration 5 (short ventilated mixer)

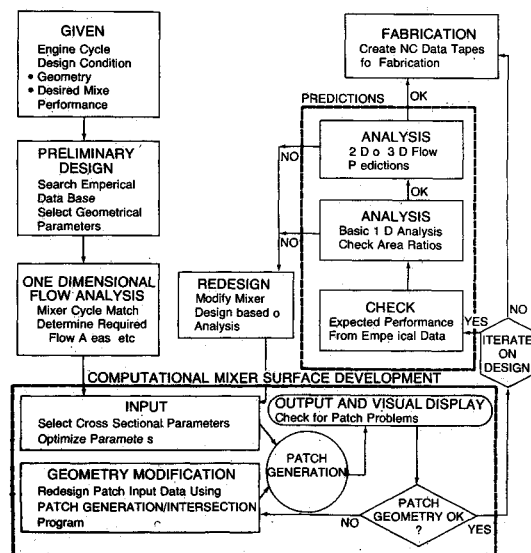


Fig 10 Summary of mixer model design procedures

temperature rake surveys at the mixing and the exhaust planes, and surface flow visualization. Before the models were mounted on the test rig, various measurement systems were leak checked and calibrated according to standard procedures. The thrust sensing system from the thrust rig NTR A was calibrated at the beginning and the end of the test using the fixed weight method. The calibration of pressure transducers and flowmeters was done prior to the beginning of the test.

A simple splitter (model Configuration 1) and a 4 in ASME nozzle were used to evaluate the mixed flow data reduction system. During the initial phase of thrust measurement, temperature and pressure distortion levels at the charging station were studied. Each performance run was repeated to serve as a double check on all measurements. A

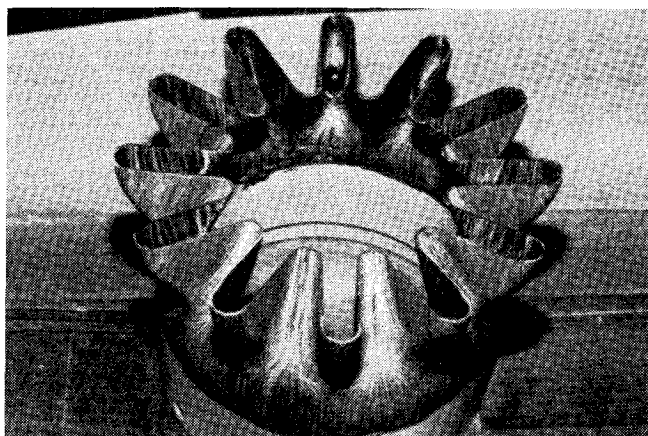


Fig. 11 Surface flow visualization pattern indicating separation on the primary side of the mixer—Configuration 3, $P_{tF}/P_a = 2.5$, $P_{tF}/P_{tP} = 1.05$, $T_{tF}/T_{tP} = 1.0$

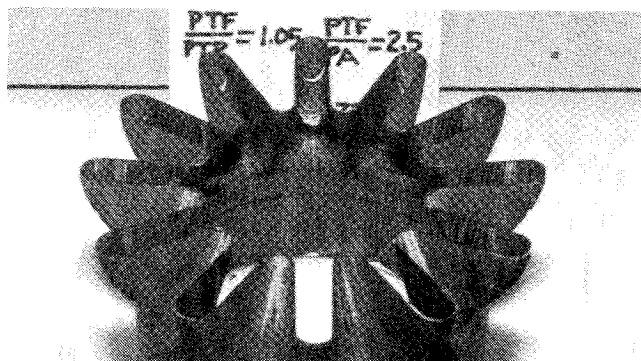


Fig. 12 Surface flow visualization pattern indicating effect of mixer ventilation—Configuration 5, $P_{tF}/P_a = 2.5$, $P_{tF}/P_{tP} = 1.05$, $T_{tF}/T_{tP} = 1.0$

“no load” thrust measurement was taken at the beginning and the end of each performance run so as to cancel out any bias errors in the thrust measurement.

All the flow visualization studies were performed during cold runs, i.e., both streams at ambient temperature. The mixer surfaces were covered evenly with the oil mixture; orange on the inside and green on the outside. The flow was then rapidly accelerated to the desired flow conditions and kept steady for at least five minutes, thus establishing the desired flow pattern while the excess oil evaporated. The matrix of test conditions is tabulated in Table 1.

Results and Discussion

Before the test results are discussed, it is important to emphasize that the basic objective of this test program was to evaluate the ventilated mixer concept in terms of overall performance characteristics. For this reason, the same mixer models were employed in the ventilated and the unventilated mixed flow test configurations so that back-to-back performance comparisons could be made. A matrix of test conditions (Table 1) was used to evaluate the effect of ventilation slots on mixer performance at various off-design flow conditions. Two mixer models of different axial lengths (Fig. 8) were selected to determine and compare 1) the effect of different degrees of flow separation on mixer performance and 2) the performance of a short ventilated mixer (Configuration 5) with respect to the performance of a long unventilated mixer (Configuration 2). The use of a short mixer would reduce the overall length of the exhaust nozzle and, hence, the weight and drag penalty on the corresponding turbofan engine.

The surface flow visualization using fluorescent oil streaks for various mixer configurations is presented in Figs. 11–13. The flow pattern shown in Fig. 11 indicates the occurrence of flow separation on the primary side of the short unventilated mixer (Configuration 3). The occurrence of flow stagnation and flow reversal can be inferred from the formation of vortices and the accumulation of oil at the center of the lobe crown. As expected, the extent of the flow separation region in the case of the long unventilated mixer (Configuration 2) is smaller. Figures 12 and 13 indicate that the flow separation, which occurred in the vicinity of the lobe crown in the unventilated mixer, is reduced or eliminated by the introduction of mixer ventilation slots. No flow separation was noticed on the fan side of any mixer configuration.

The total pressure traverse data taken at the mixing plane and the nozzle exit plane is presented in Figs. 14–16. The rake total pressures, P_{tM} and P_{tE} , have been normalized to enable comparison between different mixer configurations. The total pressure contours at the mixing plane (spanning a 30 deg sector) for mixer Configurations 3 and 5 are compared in Figs. 14 and 15. The pressure contours indicate the formation of a circulatory wake pattern, suggesting perhaps, that the mixing between the primary and the secondary streams is still

Table 1 Test conditions

Test mode	Configurations	P_{tF}/P_{tP}	T_{tF}/T_{tP}	P_{tF}/P_a
Thrust	1, 6	1.05	1.0	1.4, 2.8
		1.10	0.5	
		1.15	0.4	
Plug statics ^a	2, 3, 4, 5	1.05	1.0	1.4, 2.8
		1.10	0.5	
			0.4	
Survey	2, 3, 4, 5	1.05	0.4	1.5, 2.0, 2.5
Visualization	2, 3, 4, 5	1.05	1.0	1.5, 2.5

^a A few selected conditions only

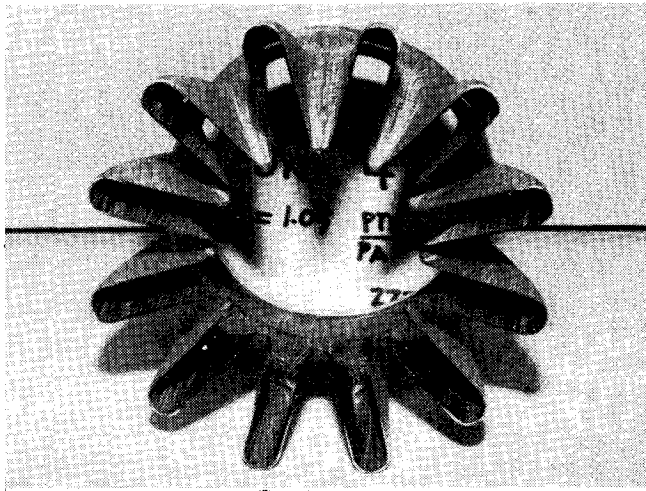
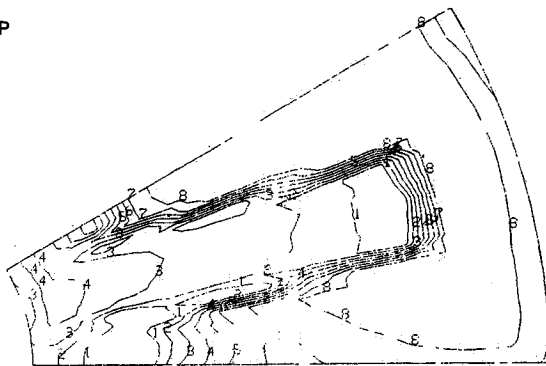


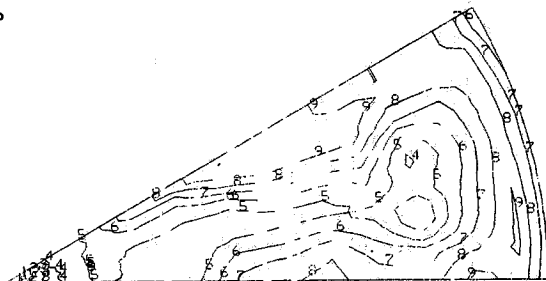
Fig. 13 Surface flow visualization pattern indicating effect of mixer ventilation—Configuration 4, $P_{tF}/P_a = 2.5$, $P_{tF}/P_{tP} = 1.05$, $T_{tF}/T_{tP} = 1.0$

PTM/PTP
1 0 98
2 0 99
3 1 00
4 1 01
5 1 02
6 1 03
7 1 04
8 1 05



(a) MIXING PLANE

PTE/PTP
1 0 97
2 0 98
3 0 99
4 1 00
5 1 01
6 1 02
7 1 03
8 1 04
9 1 05



(b) NOZZLE EXIT PLANE

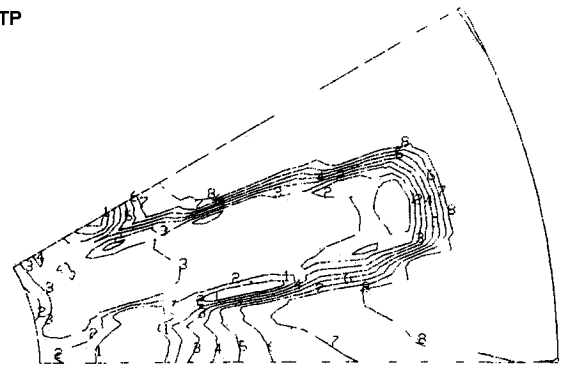
Fig. 14 Total pressure contours—Configuration 3, $P_{tF}/P_a = 2.5$, $P_{tF}/P_{tP} = 1.05$, $T_{tF}/T_{tP} = 0.4$.

in progress. The influence of lobe ventilation on the short mixer clearly reduces the total pressure loss. This conclusion is more evident from the study of total pressure profile data measured along the lobe and the valley centerlines, as Fig. 16 indicates.

Figure 17 presents the aggregate or total mixer pressure loss for both unventilated and ventilated mixer configurations. A computer program was developed to process and integrate the survey data for total values of pressures, temperatures, pressure loss, mixing effectiveness, nozzle thrust, etc. The total mixer pressure loss ($\Delta P_t/P_t$) is defined as the weighted average of the pressure loss through each passage. Thus,

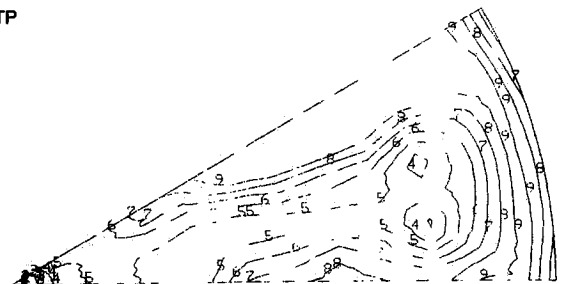
$$\left(\frac{\Delta P_t}{P_t}\right)^{\text{Mixer}} = \left\{ \left(\frac{\Delta P_t}{P_t}\right)^P W_P + \left(\frac{\Delta P_t}{P_t}\right)^F W_F \right\} / (W_P + W_F)$$

PTM/PTP
1 0 98
2 0 99
3 1 00
4 1 01
5 1 02
6 1 03
7 1 04
8 1 05



(a) MIXING PLANE

PTE/PTP
1 0 97
2 0 98
3 0 99
4 1 00
5 1 01
6 1 02
7 1 03
8 1 04
9 1 05



(b) NOZZLE EXIT PLANE

Fig. 15 Total pressure contours—Configuration 5, $P_{tF}/P_a = 2.5$, $P_{tF}/P_{tP} = 1.05$, $T_{tF}/T_{tP} = 0.4$

The results indicate that the introduction of ventilation slots causes a considerable reduction in total pressure loss through a lobe mixer. The reduction in pressure loss for the short mixer is much greater at a low fan pressure ratio, (P_{tF}/P_a) of 1.5 (about 28.5%), than at a high fan pressure ratio of 2.5 (about 16%). The corresponding reduction in total pressure loss due to ventilation slots for the long mixer is smaller; 18.1% at $P_{tF}/P_a = 1.5$ and 7.6% at $P_{tF}/P_a = 2.5$. The results also indicate that at low pressure ratios, the total pressure loss through the mixer is significantly smaller.

The total temperature contours obtained from the traverse data at the nozzle exit plane are illustrated in Fig. 18. The temperatures, T_{tM} and T_{tP} , are normalized with respect to the average primary charging station total temperature, T_{tP} . Figure 18 indicates that, although considerable temperature mixing has taken place, the pattern corresponding to the mixer lobe is still well defined at the nozzle exit plane. The slots allow secondary flow to bleed through the lobes to the primary side, and keep the boundary layer attached to the inner surface. As a consequence, this mechanism promotes additional mixing while also reducing the mixer lobe surface temperature.

The degree of mixing is indicated by a mixing effectiveness, η , defined in terms of rake survey data as

$$(\eta)_{\text{survey}} = \frac{(W_P + W_F) \sqrt{T_{tPM}} \sqrt{T_{tM}/T_{texit}} - W_P \sqrt{T_{tP}} - W_F \sqrt{T_{tF}}}{(W_P + W_F) \sqrt{T_{tM}} - W_P \sqrt{T_{tP}} - W_F \sqrt{T_{tF}}}$$

where T_{tPM} is a partially mixed exit temperature obtained by thrust averaging, T_{texit} is an energy averaged exit temperature, and T_{tM} is a fully mixed temperature based on charging station values. The mixing effectiveness, η , as a function of fan pressure ratio, P_{tF}/P_a , for various mixer configurations is presented in Fig. 19. The increase in mixing effectiveness, η , as a result of using the ventilation mixer concept, is found to be 3 to 10%.

The combined effect of total pressure loss and mixing effectiveness can be obtained from the comparison of thrust

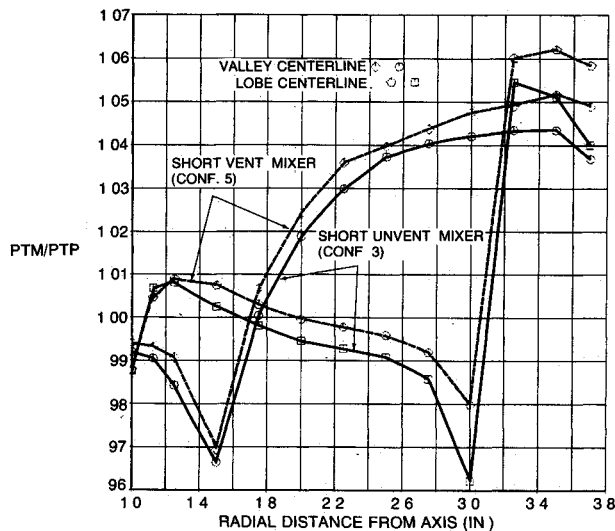


Fig 16 Mixing plane total pressure, P_{tM}/P_{tp} ; profiles at the lobe and the valley centerlines, $P_{tF}/P_a = 1.5$, $P_{tF}/P_{tp} = 1.05$, $T_{tF}/T_{tp} = 0.4$ —Configurations 3 and 5

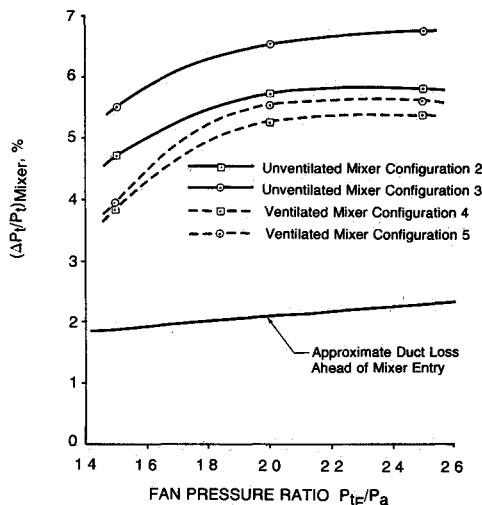


Fig 17 Mixer total pressure loss comparisons.

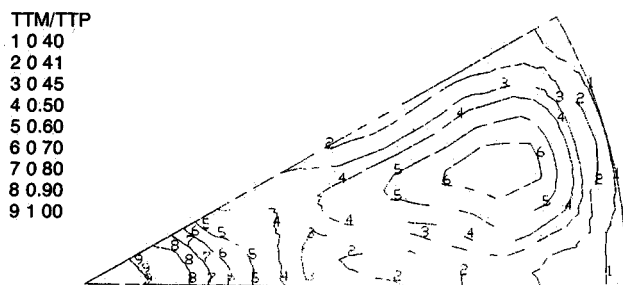


Fig 18 Total temperature contours—Configuration 5, $P_{tF}/P_a = 2.0$, $P_{tF}/P_{tp} = 1.05$, $T_{tF}/T_{tp} = 0.4$

coefficients Figure 20 presents the thrust coefficient characteristics of Configurations 3 and 5 and indicates that the ventilation increases the thrust coefficient by about 0.2%. It is important to note that, although the performance gain due to slot ventilation is small, it is significant enough when the net gain between the mixed flow engine and the separate flow engine is compared. The ventilation concept may account for up to 25% thrust improvement for the mixed flow engine.

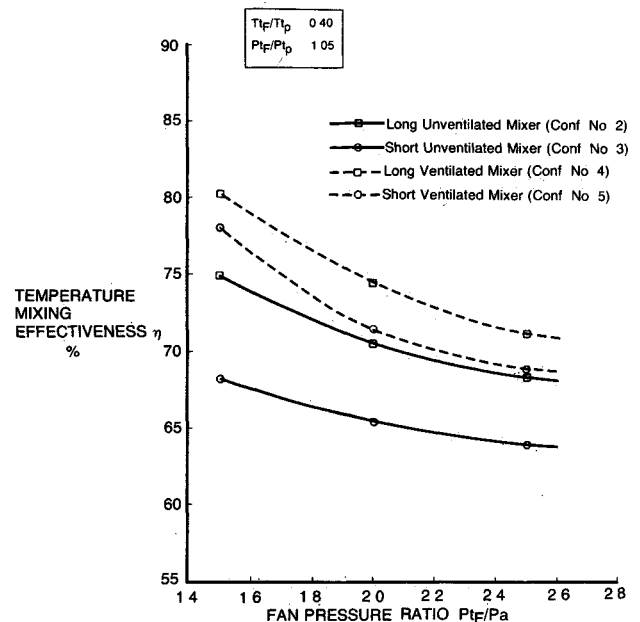


Fig 19 Temperature mixing effectiveness comparisons

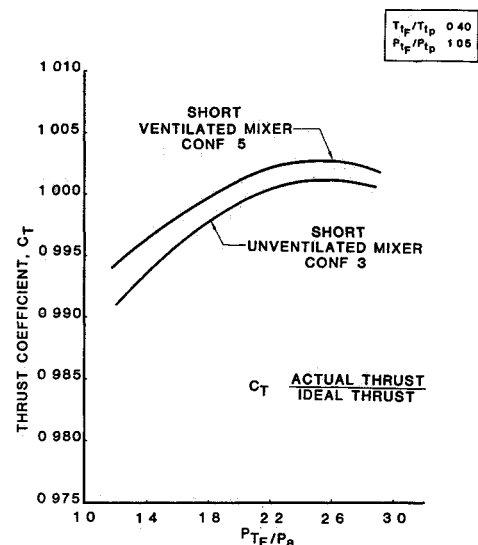


Fig 20 Comparison of thrust coefficients

To substantiate the validity of predicting mixer performance from exit survey data, a comparison between thrust calculated from exit survey data and thrust measured directly, is presented in Fig 21. It is evident that in these tests the two methods compared very well in predicting the total exhaust thrust of the mixed flow nozzle. The thrust calculated from the temperature and pressure surveys was found to be only 0.5 to 2.1% higher than that measured directly. The comparison of mixing effectiveness, η calculated by the two methods also indicated that the η based on exit survey data was consistently higher than that obtained through C_v measurement. This is due perhaps to differences in the error uncertainties in the calculation of nozzle thrust coefficients from thrust data and in the measurements of the total temperatures and pressures at the nozzle exit plane.

Finally, a trade study of the ventilated mixer on a current technology turbofan engine was conducted. The study was based on a current technology ventilated mixer with an $(L/D)_{\text{mixing}}$ of 0.65 having the same external lines as the reference annular mixer exhaust system. Although a complete

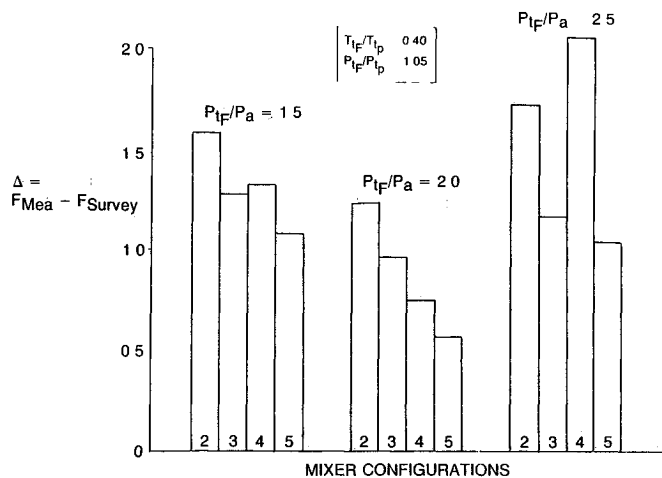


Fig. 21 Comparison of thrust calculated from exhaust survey data with directly measured thrust.

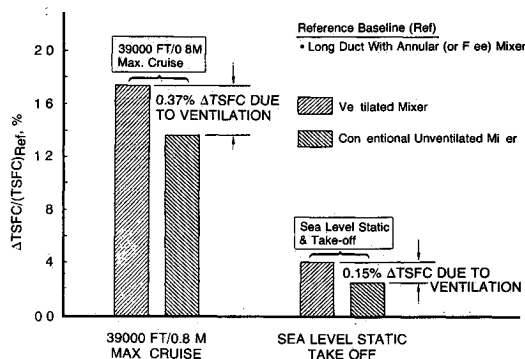


Fig. 22 Mixer internal performance estimation for a current technology turbofan engine

set of flight conditions was considered, only the takeoff and maximum cruise conditions are shown here. Performance gain is represented by a change in thrust specific fuel consumption (TSFC) with respect to an annular mixer with 25% mixing. The results are equivalent to a corresponding increase in net thrust. The results have been summarized in Fig. 22 and indicate a 0.37% TSFC improvement due to the ventilated mixer concept alone and up to 1.75% TSFC improvement over an annular or free mixer configuration having approximately the same nozzle length. It is assumed that the ventilated and the unventilated mixers have the same weight.

Noise Suppression

A HBPR jet noise suppression of the ventilated lobe mixers (Configurations 4 and 5) was conducted at the Boeing LTC facility in December 1981. Both the primary and the secondary streams were heated to simulate real engine effects. The results were compared with a new simple splitter baseline configuration. The static gas conditions tested were representative of the power settings of a current technology engine. In addition, a few test conditions were taken from the performance test (Table 1). Gas conditions were selected to represent high approach, cutback, and takeoff power levels.

The acoustic data of one-third octave band sound pressure level (1/3 OBSPL) were measured on line by an array of microphones, as illustrated in Fig. 23. The OASPL's of the long and the short ventilated mixers indicated that the noise characteristics of the two configurations were essentially the same. However, their comparison to the baseline splitter indicated considerable noise suppression. As shown in Fig.

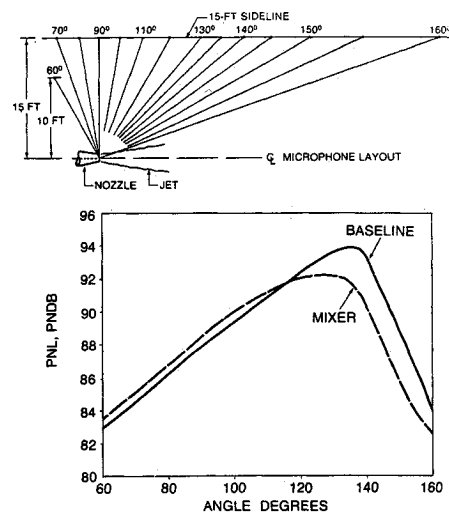


Fig. 23 Extrapolated baseline and mixer model jet noise—PNL's single engine, 1800 ft sideline, free field engine static takeoff condition, $P_{tF}/P_{tP} = 1.14$, $T_{tF}/T_{tP} = 0.445$

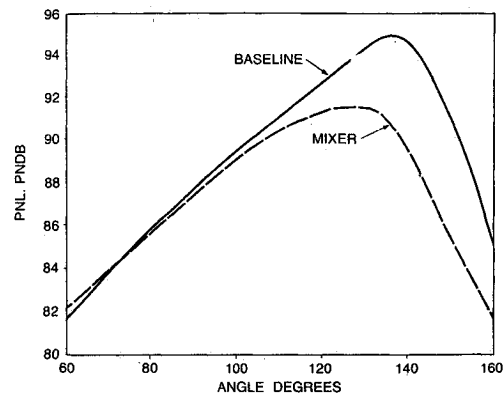


Fig. 24 Extrapolated baseline and mixer model jet noise—PNL's single engine, 1800 ft sideline, free-field engine static takeoff condition, $P_{tF}/P_{tP} = 1.05$, $T_{tF}/T_{tP} = 0.433$

23, the peak PNL suppression at the engine takeoff power condition, extrapolated to full scale (10 times) and 1800 ft sideline, is found to be 1.4 to 3 PNdB. When the pressure split P_{tF}/P_{tP} was reduced from 1.14 (takeoff condition) to 1.05, thereby decreasing the cycle bypass ratio, the noise suppression was considerably increased, as Fig. 24 indicates. This fact can be used to advantage by redesigning the ventilation slots to alter the noise and performance characteristics.

Conclusions

The major conclusions from the analysis of the test results are the following:

- 1) The ventilated mixer resulted in a significant reduction (16.29%) in total pressure loss as a result of reducing or eliminating flow separation in the primary flow. The ventilated mixer also resulted in a slight improvement (3 to 10%) in mixing effectiveness.
- 2) For a current technology high bypass turbofan engine, the combined effect of ventilated mixer is found to give 0.4% gain in TSFC over the corresponding unventilated mixer.
- 3) A separate noise suppression test indicated that the ventilated mixer had a higher noise reduction potential (1.4 to 3 PNdB) than an annular or free mixer.

4) The performance of the ventilated short mixer is greater than that of the unventilated long mixer. Thus, the mixer length and, hence, the overall nozzle length of the exhaust system, can be reduced by using this concept for equal performance gain.

It is possible to further improve the performance of these mixers by redesigning and sizing the ventilation slots to a particular design application and test condition.

References

- ¹Kuchar, A. P. and Chamberlin, R., 'Scale Model Performance Test Investigation of Exhaust System Mixers for an Energy Efficient Engine (E³) Propulsion System', AIAA Paper 80-0229, Jan 1980.
- ²Kozlowski, H. and Kraft, G., 'Experimental Evaluation of Exhaust Mixers for an Energy Efficient Engine', AIAA Paper 80-1088, June 1980.
- ³McComb, J. G., Parsons, S. V., and Wilson, J. A., 'Exhaust System Performance Improvement for a Long Duct Nacelle Installation for the DC 10', AIAA Paper 80-1195, June 1980.
- ⁴Shumpert, P. K., 'An Experimental Model Investigation of Turbofan Engine Internal Exhaust Gas Mixer Configuration', AIAA Paper 80-0228, Jan 1980.
- ⁵Sokhey, J. S. and Farquhar, B. W., 'Ventilated Mixer', Patent Disclosure 79-326, Dec 1979.
- ⁶Crowder, J. P., Hill, E. G., and Pond, C. R., 'Selected Wind Tunnel Testing Developments at the Boeing Aerodynamics Laboratory', AIAA Paper 80-0458, CP, March 1980.
- ⁷Gibson, S. G., 'User's Manual for MASTER: The Modeling of Aerodynamic Surfaces by Three Dimensional Explicit Representation', NASA CR 166056, Jan 1983.

From the AIAA Progress in Astronautics and Aeronautics Series . . .

RADIATION ENERGY CONVERSION IN SPACE—v 61

Edited by Kenneth W. Billman, NASA Ames Research Center, Moffett Field, California

The principal theme of this volume is the analysis of potential methods for the effective utilization of solar energy for the generation and transmission of large amounts of power from satellite power stations down to Earth for terrestrial purposes. During the past decade, NASA has been sponsoring a wide variety of studies aimed at this goal—some directed at the physics of solar energy conversion, some directed at the engineering problems involved, and some directed at the economic values and side effects relative to other possible solutions to the much discussed problems of energy supply on Earth. This volume constitutes a progress report on these and other studies of SPS (space power satellite systems) but more than that the volume contains a number of important papers that go beyond the concept of using the obvious stream of visible solar energy available in space. There are other radiations, particle streams, for example, whose energies can be trapped and converted by special laser systems. The book contains scientific analyses of the feasibility of using such energy sources for useful power generation. In addition, there are papers addressed to the problems of developing smaller amounts of power from such radiation sources by novel means for use on spacecraft themselves.

Physicists interested in the basic processes of the interaction of space radiations and matter in various forms, engineers concerned with solutions to the terrestrial energy supply dilemma, spacecraft specialists involved in satellite power systems, and economists and environmentalists concerned with energy will find in this volume many stimulating concepts deserving of careful study.

690 pp., 6×9 illus. \$24.00 Mem. \$45.00 List

TO ORDER WRITE: Publications Dept. AIAA, 1290 Avenue of the Americas, New York, N.Y. 10019